

Finite Element Analysis of Changes in Deformation of Intraocular Segments by Airbag Impact in Eyes of Various Axial Lengths

Tomohiro Ueno , Hideaki Fujita , Aya Ikeda, Kazuhiro Harada , Tomoko Tsukahara-Kawamura , Hiroaki Ozaki, Eiichi Uchio 

Department of Ophthalmology, Fukuoka University School of Medicine, Fukuoka, Japan

Correspondence: Eiichi Uchio, Department of Ophthalmology, Fukuoka University School of Medicine, 7-45-1 Nanakuma, Jonan-ku, Fukuoka, 814-0180, Japan, Tel +81 92 801 1011, Fax +81 92 865 4445, Email euchio@fukuoka-u.ac.jp

Background: We studied the kinetic phenomenon of an airbag impact on eyes with different axial lengths using finite element analysis (FEA) to sequentially determine the physical and mechanical responses of intraocular segments at various airbag deployment velocities.

Methods: The human eye model we created was used in simulations with the FEA program PAM-GENERIS™. The airbag was set to impact eyes with axial lengths of 21.85 mm (hyperopia), 23.85 mm (emmetropia) and 25.85 mm (myopia), at initial velocities of 20, 30, 40, 50 and 60 m/s. The deformation rate was calculated as the ratio of the length of three segments, anterior chamber, lens and vitreous, to that at the baseline from 0.2 ms to 2.0 ms after the airbag impact.

Results: Deformation rate of the anterior chamber was greater than that of other segments, especially in the early phase, 0.2–0.4 ms after the impact ($P < 0.001$), and it reached its peak, 80%, at 0.8 ms. A higher deformation rate in the anterior chamber was found in hyperopia compared with other axial length eyes in the first half period, 0.2–0.8 ms, followed by the rate in emmetropia ($P < 0.001$). The lens deformation rate was low, its peak ranging from 40% to 75%, and exceeded that of the anterior chamber at 1.4 ms and 1.6 ms after the impact ($P < 0.01$). The vitreous deformation rate was lower throughout the simulation period than that of the other segments and ranged from a negative value (elongation) in the later phase.

Conclusion: Airbag impact on the eyeball causes evident deformation, especially in the anterior chamber. The results obtained in this study, such as the time lag of the peak deformation between the anterior chamber and lens, suggest a clue to the pathophysiological mechanism of airbag ocular injury.

Keywords: airbag, ocular trauma, computer simulation, lens, anterior chamber, vitreous body, finite element analysis, deformation

Introduction

Automotive safety devices have measurably reduced morbidity and mortality associated with motor vehicle accidents.¹ However, airbags have been recognized as a potential cause of various fatal and nonfatal injuries to the head, eyes, neck, chest, and arms.^{2,3} Because airbags are deployed at velocities of up to 200 mph, significant injury may occur if the occupant comes into contact with the airbag during the inflation phase. Most ocular injuries associated with airbags are minor. However, serious and visually devastating ocular injuries caused by airbags, ranging from corneal endothelial cell loss to retinal detachment, have been reported.^{4–16} Minor ocular injuries due to airbag impact include corneal abrasion, hyphema, vitreous hemorrhage, retinal tear, maculopathy, and localized photoreceptor damage.^{8,16–21} Moderate to serious ocular injuries include corneoscleral laceration, bullous keratopathy, lens dislocation, lens capsule rupture, choroidal rupture, retinal detachment, and open globe rupture.^{6,7,9,12,15,22–26} Mohamed et al reported that self-limiting injuries occurred at low velocity (10–30 mph).²⁷ It was thought that, at low velocities, there may be a delay before the sensors transmit the firing

signal, causing the airbag to strike the occupant while it continues to expand, resulting in moderate-to-severe ocular injury in relatively low-velocity crashes in which the airbag was fully deployed.²⁷

The mechanisms that induce intraocular damage and influence the severity of airbag ocular injuries have been reported in a restricted number of studies. Duma et al used human cadaver eyeballs, which were impacted in situ after being repressurized with saline injected through a 30-gauge needle, and observed that all the eyes revealed detached retinas.²⁸ Injury determination was achieved by ophthalmic ultrasound imaging, staining with fluorescein dye, and dissection.²⁸ The impact velocities of the airbags ranged from 30 to 66 m/s.²⁸ The same group carried out experiments using porcine eyes as a model of the human eye impacted by a pneumatic cannon designed to propel foam objects at velocities ranging between 20 and 100 m/s, and found that even in the worst-case scenario, the most severe observed injury was corneal abrasion.²⁹ Biomechanical approaches are now feasible and can considerably help experts to investigate the issue without ethical concerns. Shirzadi et al developed a finite element (FEA) model of the eye and performed simulation of an airbag impact on the eyeball and determined the stress and strain contours at 0.3 ms after eye-airbag impact with a velocity of 67 m/s.³⁰ The sclera, ciliary body, cornea, and lens were the eye segments with the highest stress (maximum stress reached 9.3 MPa), whereas the cornea, retina, and choroid experienced the highest strain (maximum of 14.1%).³⁰

As shown above, only a few studies have evaluated the clinicopathological mechanism of airbag ocular injuries, especially in a simulation model.^{30,31} We have previously developed a simulation model resembling a human eye and applied 3-dimensional FEA to determine the physical and mechanical conditions of impacting foreign bodies that cause an intraocular foreign body.³² This model human eye was also used in our studies on airbag impact in various situations.^{33–38} We applied this FEA model and reported that considerable damage was observed especially at higher impact velocities, such as 50 or 60 m/s, in eyes with any axial length, and deformation was most evident in the anterior segment.³⁹ In these studies, we mainly reported mechanical damage of the ocular surface, such as laceration, perforation, etc., and deformation of the whole eyeball was evaluated, but intraocular deformation, which is closely related to angle recession, lens rupture and vitreous traction etc., was not evaluated.

From these studies on eye-airbag injury, it remains to be determined how each ocular segment undergoes deformation during the airbag impact process. This is closely related to the pathophysiological mechanism that induces severe ocular trauma, resulting in a poor visual prognosis. Therefore, we planned to study the kinetic phenomenon of airbag impact on eyes with different axial lengths, using an FEA method to determine the physical and mechanical responses of intraocular segments sequentially at various airbag deployment velocities, particularly to survey the axial deformation rate of each segment, which cannot be evaluated even in animal experiments. If we were able to obtain any information regarding the kinetic response of each segment during the critical period of airbag deployment, this might enable us to more precisely understand the mechanism of ocular damage due to airbag impact on the eye.

Materials and Methods

A model human eye was used in simulations with a computer using the FEA program PAM-GENERISTM (Nihon ESI, Tokyo, Japan).³² The model of the human eye is composed of three layers: outer (cornea and sclera), middle (iris, ciliary body, choroid, and retina), and inner (aqueous humor, lens, and vitreous), as reported previously (Table 1).³² The eyelid

Table 1 Number and Property of Meshes Used for FEA Model

Anatomic Component	Shell	Solid
Cornea	380	0
Sclera	1580	0
Iris, ciliary body and choroid	1040	0
Lens	680	0
Aqueous humor	0	288
Vitreous	0	2664
Total	3680	2952

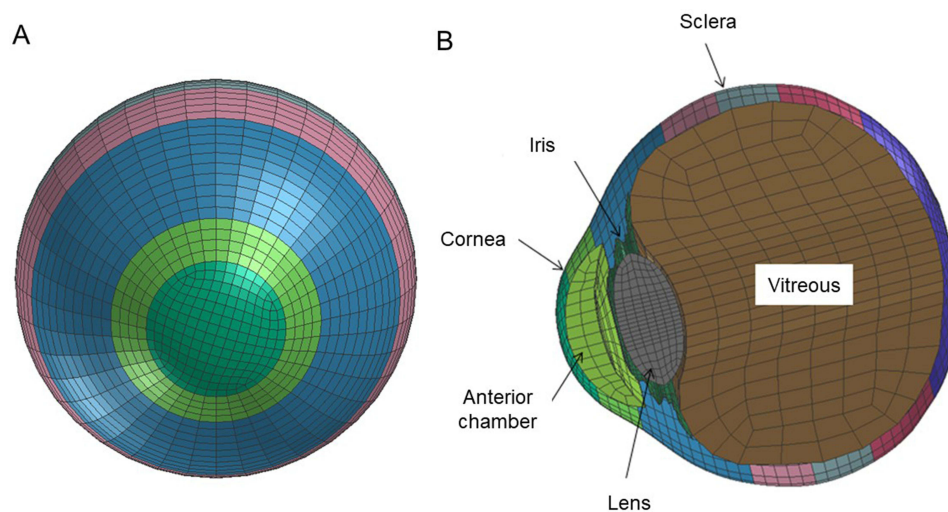


Figure 1 Frontal (A) and sagittal (B) view of model eye of emmetropia.

and orbital bone were not included in this simulation, for simplification. The depth of the anterior chamber was assumed to be 2.95 mm, which was simulated as a solid element. The lens was assumed to be biconvex and was designed as a shell element. The vitreous length was assumed to be 16.65 mm, and the posterior curvature of the retina was assumed to be 12.0 mm in the emmetropic eye model.³² Vitreous was modeled as a solid mass with a hydrostatic pressure of 20 mmHg (2.7 kPa).^{37,38} To our knowledge, there are no published data on the mechanical properties, especially on the tensile strength, of the zonule of Zinn, and thus, the suspensory ligaments and ciliary muscles are not included in this model. The elastic properties and meshing principles of the model human normal eye (emmetropia) were similar to those in previous reports.^{36,39} A revision in this study was the addition of a condition in the model human eyes with complete adhesion between the layers, the outer layer (cornea and sclera) and inner layer (anterior chamber, lens and vitreous) including the middle layer, to represent the clinical situation more accurately (Figure 1). The mass densities of ocular tissues were derived from past reports and assumed to be as follows: cornea, 1.149 g/cm³; sclera, 1.243 g/cm³; vitreous, 1.002 g/cm³; aqueous humor, 1.000 g/cm³.³⁴

We replaced the head of the dummy with a biomechanical model of the head in which the eyeball model was inserted to modify the Hybrid III model⁴⁰ for the simulation. Poisson ratio of the cornea of 0.420 and the sclera of 0.470 were used to determine the standard stress-strain curves for cornea and sclera.^{41,42} It is reported that the normal axial length ranges from 22 to 24.5 mm.⁴³ Different axial lengths, representing a normal eye with normal axial length of 23.85 mm, a hyperopic eye with a shorter axial length of 21.85 mm, and a myopic eye with a longer axial length of 25.85 mm, were used as in our previous study.^{38,39} Length or thickness of the intraocular segments in the axial direction in the three axial length eye models is shown in Table 2. Ocular elements in each model were shortened or elongated according to the proportion versus the normal eye in the optical axis direction; however, the diameters in the frontal view and the total volume of the cornea and sclera were assumed

Table 2 Length or Thickness of Intraocular Segments in Axial Direction at Baseline of Three Axial Length Eye Models

Anatomic Component	Myopic Eye	Emmetropic Eye	Hyperopic Eye
Cornea	0.49 (mm)	0.45	0.41
Anterior chamber	3.19	2.95	2.71
Lens	4.12	3.80	3.48
Vitreous	18.05	16.65	15.25
Total length	25.85	23.85	21.85

to be constant.³² Deformation of the eyeball in the axial view was displayed sequentially in slow motion. The axial deviation from the original point (before the airbag impact) was displayed sequentially by color mapping.

The impact velocity of airbags has been reported to range from 100 to 200 mph, with an average velocity of 144 mps (64.5 m/s).⁴⁴ Airbag deployment velocities have been calculated physically in the range from 100 to 300 km/h (approximately 28 to 83 m/s).⁴⁵ According to these data, different velocities, 20, 30, 40, 50 and 60 m/s, were applied in the forward direction in this study. The most important difference between our model and a similar FE study conducted by Shirzadi et al,³⁰ in which they thoroughly evaluated the stress–strain curve of ocular tissues, was the consecutive intraocular segment deformation analysis. The eye segments were divided into three segments: anterior chamber, lens, and vitreous. Corneal thickness was included in the anterior chamber. The deformation rate was calculated as the ratio of each segment to the baseline by measuring the length or thickness of each segment in the axial sectional view. It was reported that the time when peak stress emerged in eye segments in airbag ocular injury was 0.3 ms,^{8,30} however, we calculated the deformation rate from 0.2 to 2.0 ms, the final simulation time in this study, for precise evaluation to find the true moment of peak deformation. Regarding time-step size, this depends on the size of elements and material property values. In our human eye FEA model, time-step size was 0.000185 ms in average. However, due to its enormous volume of results, the results in this study were output in 0.2 ms interval.

The mean deviation in the five simulation situations was considered as the deviation of each segment. One-way ANOVA with Tukey–Kramer test was conducted to identify differences among the deformation rates for the same situation, same time after the impact, and same airbag impact velocity. GraphPad Prism9J (MDF Co., Ltd., Tokyo, Japan) was used for statistical analysis. A P-value of <0.05 was accepted as statistically significant.

Results

Axial views of each eye length at five different airbag impact velocities are displayed sequentially at 0.2-ms intervals in [Figure 2](#) (hyperopia), [Figure 3](#) (emmetropia), and [Figure 4](#) (myopia). For example, [Figure 2A–E](#) show the results for the impact velocities of 20, 30, 40, 50, and 60 m/s, respectively. However, we obtained abundant images, and thus, the results at 0, 0.2, 0.8, 1.4 and 2.0 ms after the impact are displayed. From the overview observation, after the initiation of airbag impact, depression of the cornea was firstly observed, followed by shallowing of the anterior chamber. Lenticular deformation was observed after these events; thereafter, a gradual change in vitreous depth was observed.

The deformation rates of the length or thickness of the three intraocular segments, anterior chamber, lens and vitreous are displayed on a line graph in which the deformation rates of each segment for the three eye lengths are shown in each color at different impact velocities ([Figures 5–14](#)). The blue, yellow and red lines represent the deformation rates of the anterior chamber, lens and vitreous, respectively. The solid, dashed, and dash-dotted lines represent the deformation rates for emmetropia, hyperopia, and myopia, respectively ([Figures 5–14](#)). In the early phase after the impact, 0.2–0.4 ms, deformation of the anterior chamber (blue lines) was greater than that of other segments ($P < 0.001$, [Figures 5–7](#)). The value reached its peak, 80%, at 0.8 ms ([Figure 8](#)), and after that point, the deformation rate of the anterior chamber decreased ([Figures 9–14](#)). Higher deformation rate of the anterior chamber was found in hyperopia compared with other axial length eyes in the first half period, 0.2–0.8 ms, and a significant difference was observed among different axial lengths especially at all impact velocities at 0.2–0.4 ms after the impact ($P < 0.001$).

Deformation rate of the lens was low while that of the anterior chamber was high, at 0.2–1.2 ms after the impact ([Figures 5–10](#)). Deformation rate of the lens exceeded that of the anterior chamber in 30 m/s impact at 1.2, 1.4 and 1.6 ms after the impact ($P < 0.01$) ([Figures 10–12](#)). The highest deformation rate of the lens ranged from 30 to 40%. This means that shallowing of the anterior chamber did not directly compress the lens, but the thickness of the lens decreased at an interval (0.4–0.6 ms) after the peak deformation of the anterior chamber.

The vitreous deformation rate was lower throughout the simulation period, and the values of the three axial lengths showed less variation than those of the anterior chamber or lens. It seems evident that the deformation

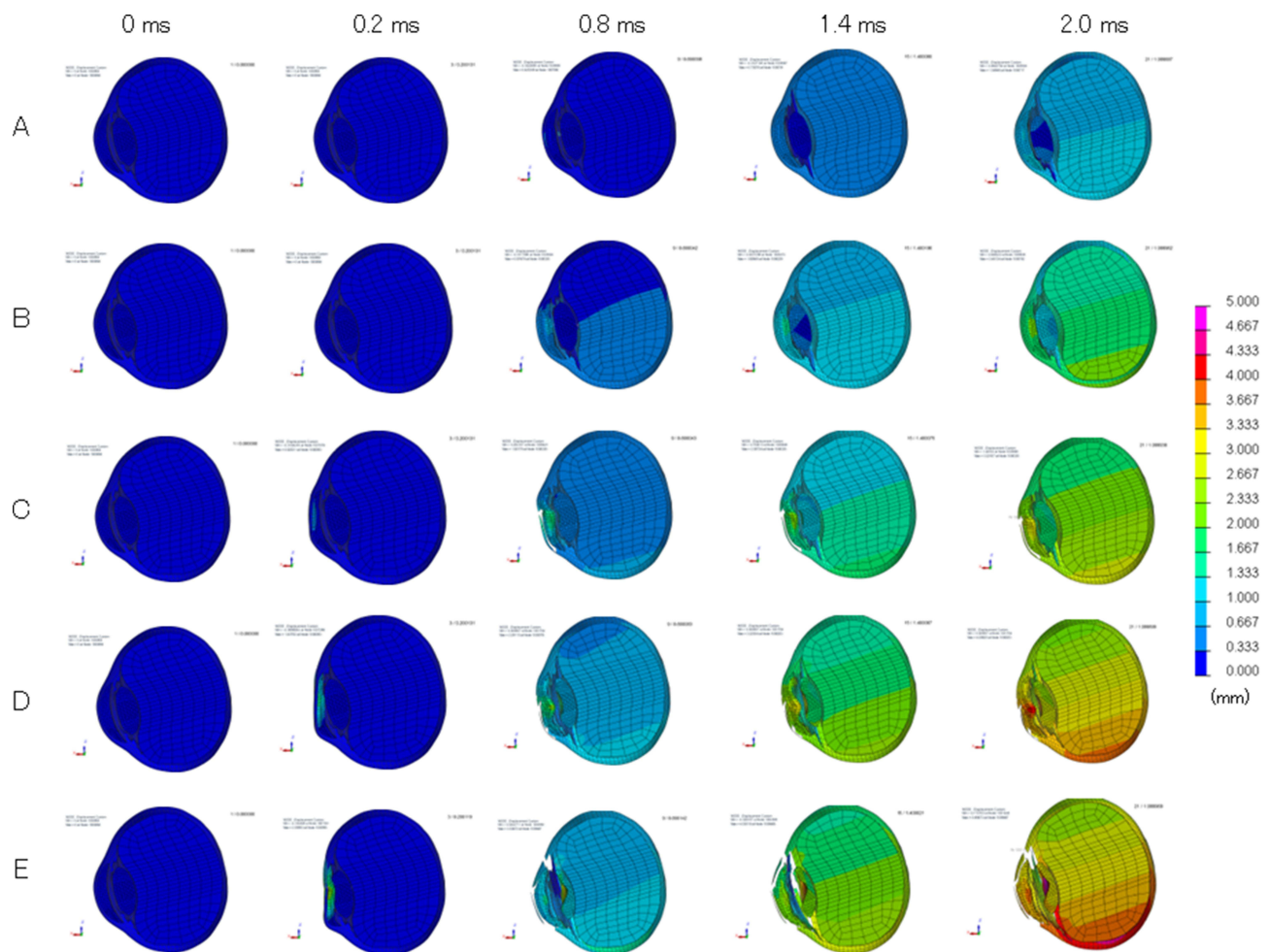


Figure 2 Sequential deformity of hyperopic eye upon airbag impact at five different velocities. Cases of impact velocities of 20 (A), 30 (B), 40 (C), 50 (D), and 60 m/s (E) in the normal-length model eye are shown. Results at 0, 0.2, 0.8, 1.4 and 2.0 ms after the impact are displayed. Axial deviation from the baseline position is displayed in each figure on a color-bar scale.

rate of the vitreous ranged from a negative value (elongation) in the later phase, after 1.4 ms (Figures 11–14), indicating that deformation of the vitreous occurred later following lens deformation.

Discussion

We previously reported that considerable damage, such as corneal or scleral laceration, has been observed, especially at higher airbag impact velocities, such as 50 or 60 m/s, at any axial length (emmetropia, hyperopia, and myopia).³⁹ The important novelty of this study compared to past simulation studies on blunt ocular trauma^{30,31} is that deformation of the intraocular segments was evaluated in detail in this study. Considering the higher energy induced by a greater airbag impact velocity, the results of this study showed that the deformation rate increased with an increase in impact velocity at each time point. Pearlman et al reported that damage to the anterior structures is most common with blunt or contusive force, and posterior segment trauma is less common.⁴⁶ It is also reasonable that the deformation rate of the anterior segment was higher than that of the posterior segment, because the anterior chamber is located in the anatomically most forward position, adjacent to the cornea. We found that deformation of the anterior chamber (blue lines) was greater than that of other segments in the early phase after the impact (0.2–0.4 ms) and that it peaked at 0.8 ms (Figure 8). Although several cases of severe blunt trauma to the anterior chamber have been reported,^{7,8,16,17,22} it is impossible to

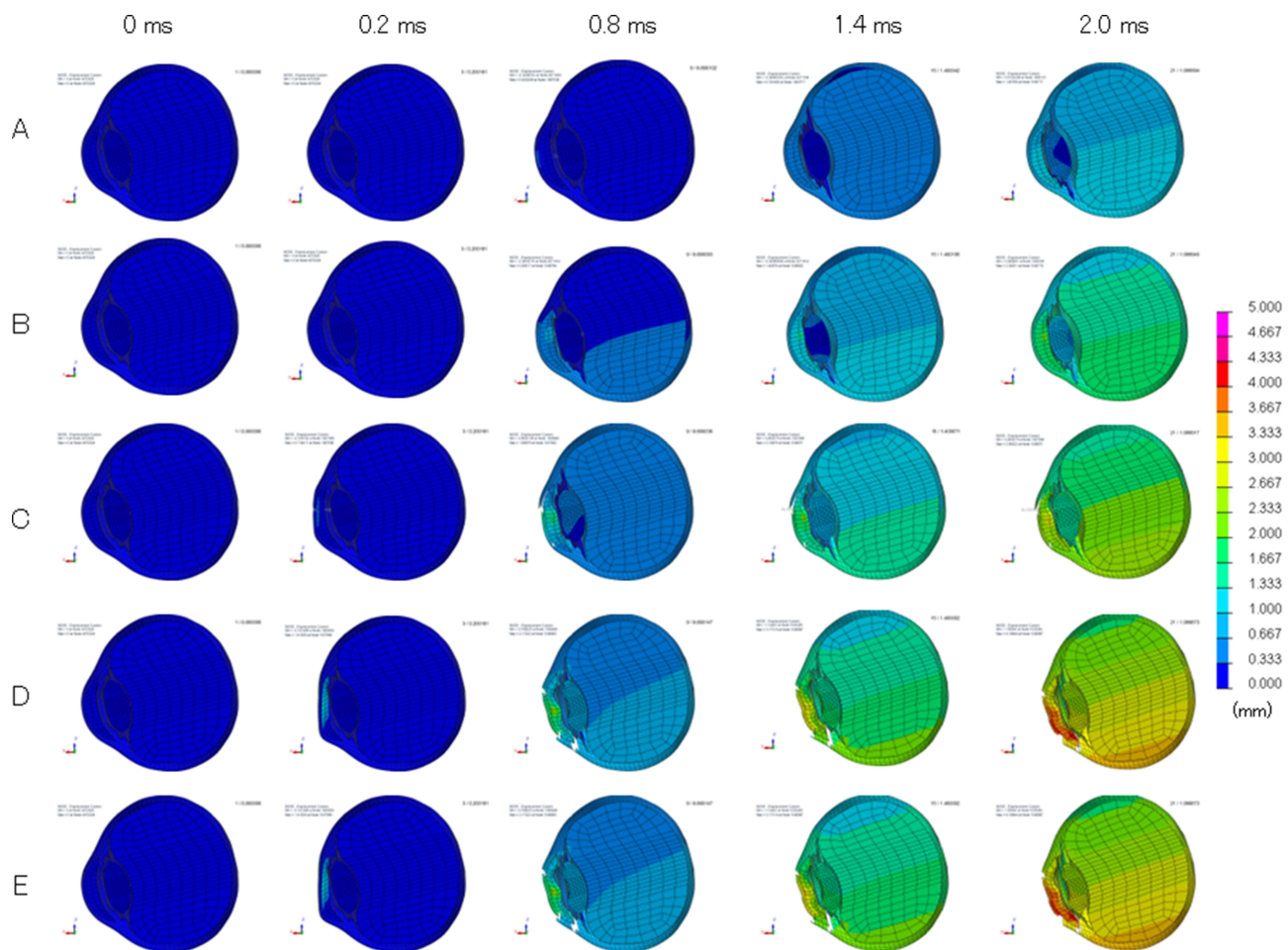


Figure 3 Sequential deformity of emmetropic eye upon airbag impact at five different velocities. Cases of impact velocities of 20 (A), 30 (B), 40 (C), 50 (D), and 60 m/s (E) in the normal-length model eye are shown. Results at 0, 0.2, 0.8, 1.4 and 2.0 ms after the impact are displayed. Axial deviation from the baseline position is displayed in each figure on a color-bar scale.

determine what occurred inside the anterior chamber and how the deformation of the anterior chamber occurred during the critical moment. In this study, it was also indicated that the deformation rate of the anterior chamber was highest in hyperopic eyes compared with other axial length eyes throughout almost the entire observation period, and the rate in emmetropia was the second highest. As this kind of minute analysis has not been reported previously, our results may provide a clue for future refinement to decrease the risk of anterior chamber decompression by modifying the deployment movement during the very early phase of airbag deployment.

It has been reported that the majority of cases of cataract following airbag injury were due to opacification of the anterior capsule and cortex, possibly because of contact between the corneal endothelium and the anterior lens surface.⁴⁷ This kind of serious deformity in the anterior chamber–lens interaction could be observed, especially in the middle to late phase of higher velocity impact in our simulation (Figures 2E, 3E and 4E). The result that the deformation rate of the lens exceeded that of the anterior chamber at 0.4 ms at 60 m/s airbag-impact velocity (Figure 6) might have some relationship with several clinical reports regarding lens blunt damage in airbag ocular injury.^{23,24} However, it should be noted that collision between the airbag and the eye in severe blunt trauma results in indentation of the cornea, a reduction in anterior-posterior diameter of the globe, and horizontal expansion of the equatorial zone after lens decompression, based on the report by Stein et al.⁴⁷ Collectively, it can be considered that the lens has an important mechanical role during the middle phase of airbag ocular injury through its movement onto the posterior segment.

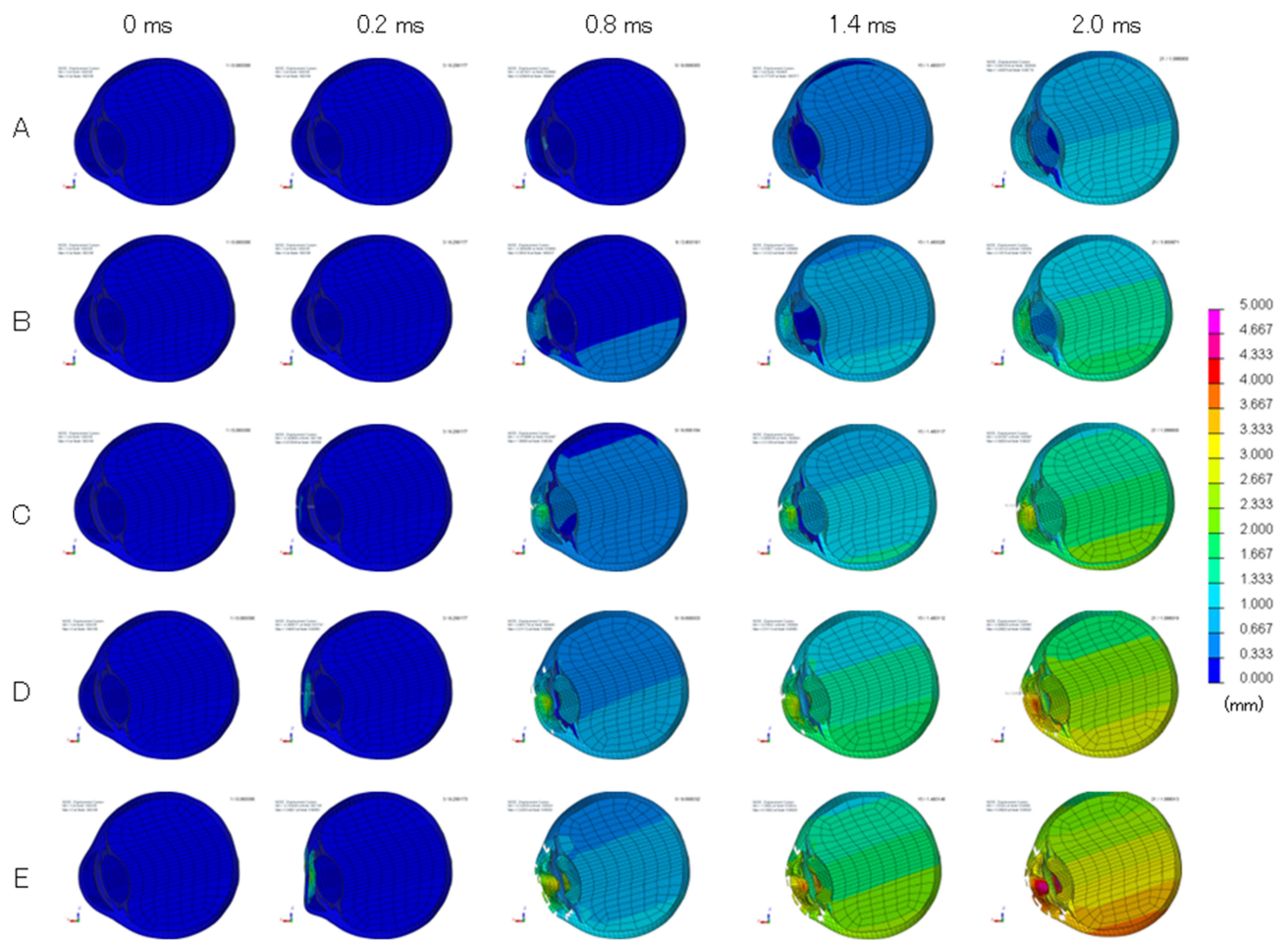


Figure 4 Sequential deformity of myopic eye upon airbag impact at five different velocities. Cases of impact velocities of 20 (A), 30 (B), 40 (C), 50 (D), and 60 m/s (E) in the normal-length model eye are shown. Results at 0, 0.2, 0.8, 1.4 and 2.0 ms after the impact are displayed. Axial deviation from the baseline position is displayed in each figure on a color-bar scale.

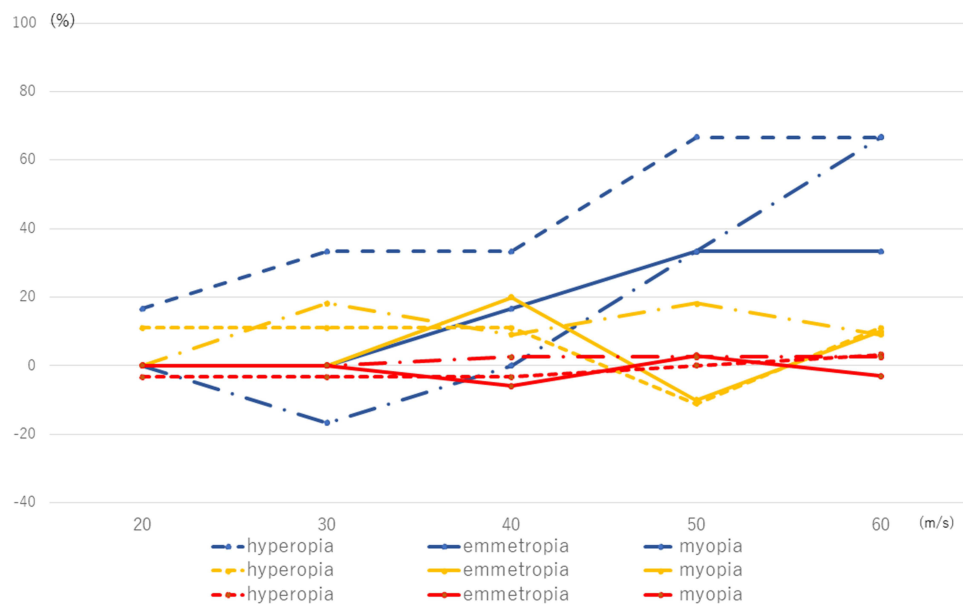


Figure 5 Deformation rate of anterior chamber, lens and vitreous for eyes with three axial lengths at 0.2 ms after airbag impact at five impact velocities. Deformation rates of the anterior chamber, lens, and vitreous are represented by blue, yellow and red lines, respectively. Solid, dashed, and dash-dotted lines represent the deformation rates of emmetropia, hyperopia, and myopia, respectively.

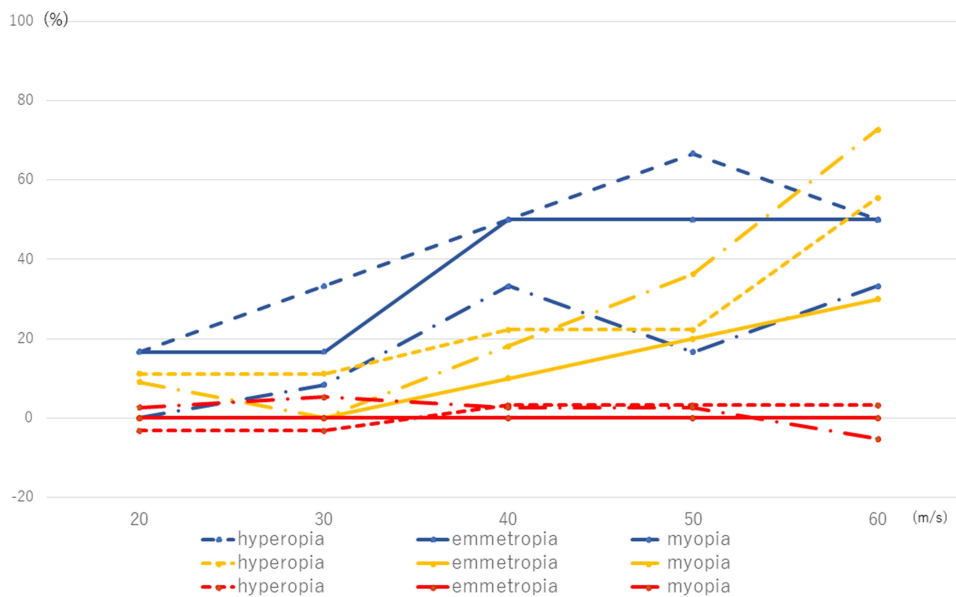


Figure 6 Deformation rate of anterior chamber, lens and vitreous for eyes with three axial lengths at 0.4 ms after airbag impact at five impact velocities. Legends pertaining to the line drawings are the same as in Figure 5.

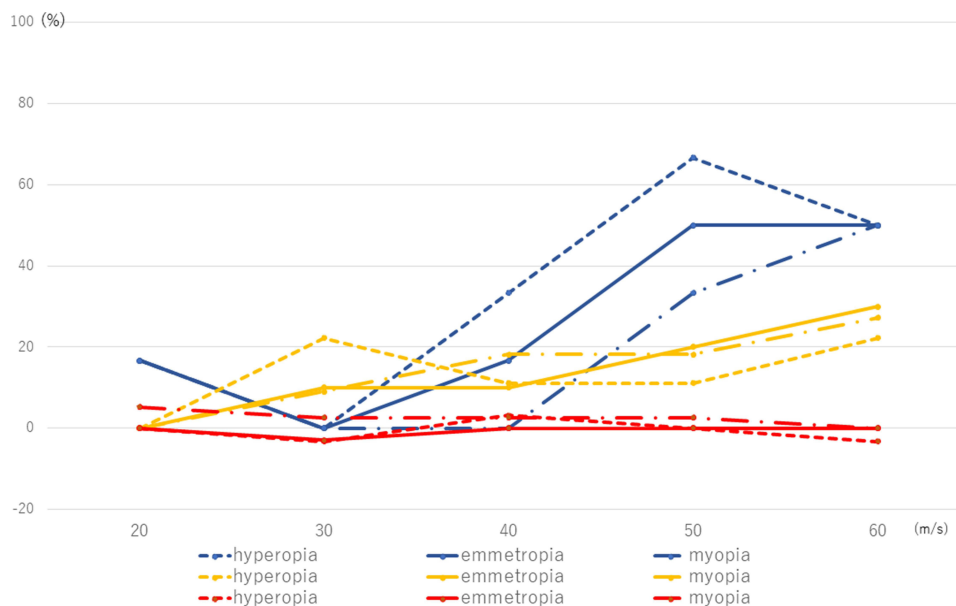


Figure 7 Deformation rate of anterior chamber, lens and vitreous for eyes with three axial lengths at 0.6 ms after airbag impact at five impact velocities. Legends pertaining to the line drawings are the same as in Figure 5.

Despite the relatively rare occurrence of vitreoretinal complications with airbag impact, there are a wide variety of clinical presentations of this disorder, such as vitreous hemorrhage,⁴⁸ retinal tear,^{18,20} retinal detachment,⁹ choroidal rupture¹⁵ and macular disorders.^{21,49} Severe blunt trauma has been shown to decrease the anterior-posterior diameter of the globe by 41%.⁵⁰ Severe traction on the vitreous base develops during the initial phase following impact.⁵¹ Stein et al⁴⁷ therefore theorized that the vitreous is slower to respond to the sudden change in globe contour and that traction is created at the vitreous base, indicating that there is expansion of the equatorial diameter of the globe. It was reported by Shirzadi et al, in a biomechanical simulation study of eye-airbag impacts, that the highest strain occurred in the cornea with a maximum of about 14.1%, and choroid

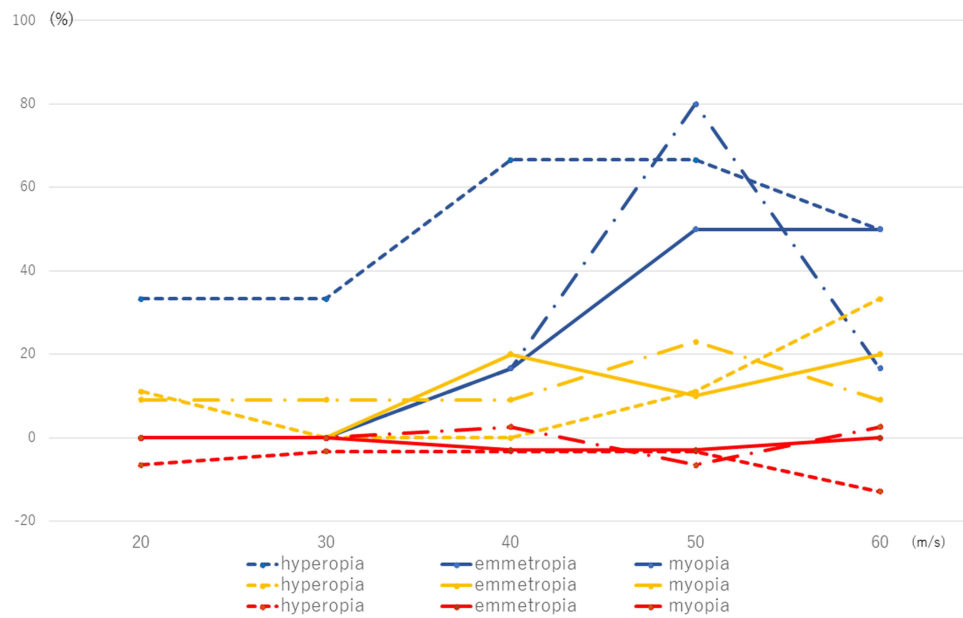


Figure 8 Deformation rate of anterior chamber, lens and vitreous for eyes with three axial lengths at 0.8 ms after airbag impact at five impact velocities. Legends pertaining to the line drawings are the same as in Figure 5.

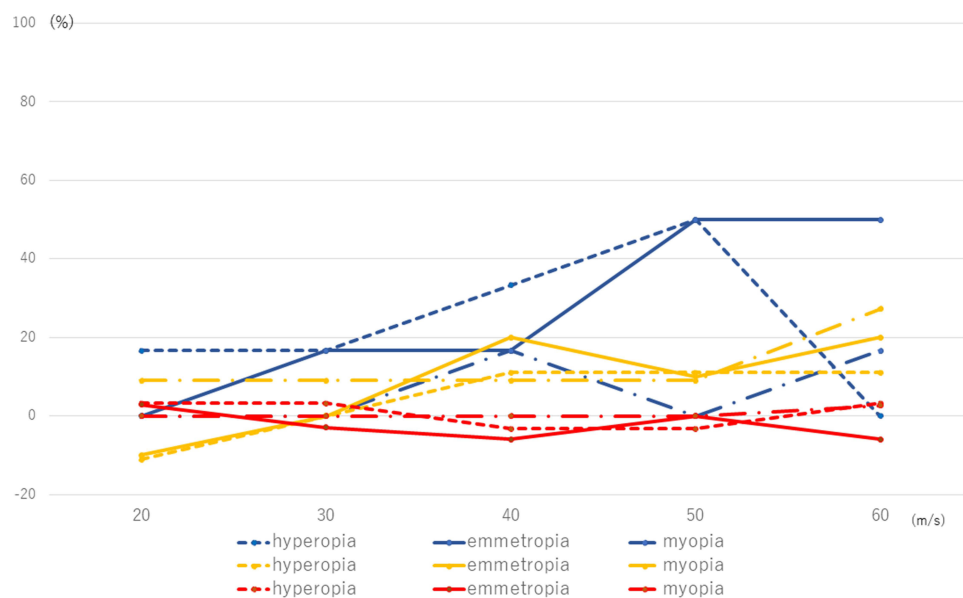


Figure 9 Deformation rate of anterior chamber, lens and vitreous for eyes with three axial lengths at 1.0 ms after airbag impact at five impact velocities. Legends pertaining to the line drawings are the same as in Figure 5.

(12.8%) and retina (12.4%) were other segments with high strain.³⁰ This result of ocular outer surface strain suggests that the retina or choroid might suffer the greatest damage, resulting in sight-threatening complications reported previously.^{9,15,49} Deformation rate of the vitreous was very low, and the vitreous might act as a shock absorber against the deformation caused by the anterior segment due to its large volume. However, an interesting tendency was that vitreous length showed elongation in the later phase of airbag impact in our study. The traction created at the vitreous base by expansion of the equatorial diameter of the globe due to airbag impact is the main factor in vitreoretinal complications of airbag ocular injury, as proposed by Stein et al.⁴⁷ Our finding

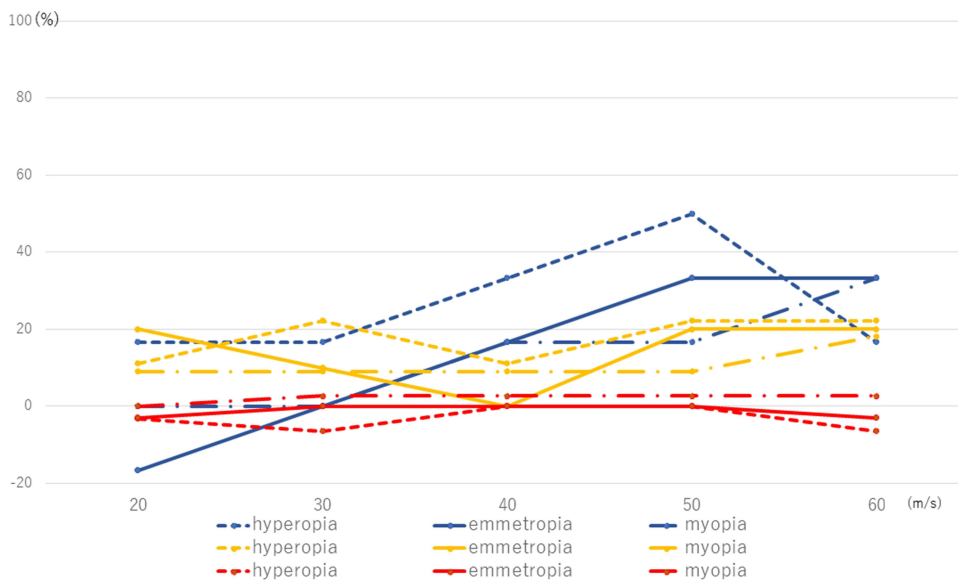


Figure 10 Deformation rate of anterior chamber, lens and vitreous for eyes with three axial lengths at 1.2 ms after airbag impact at five impact velocities. Legends pertaining to the line drawings are the same as in Figure 5.

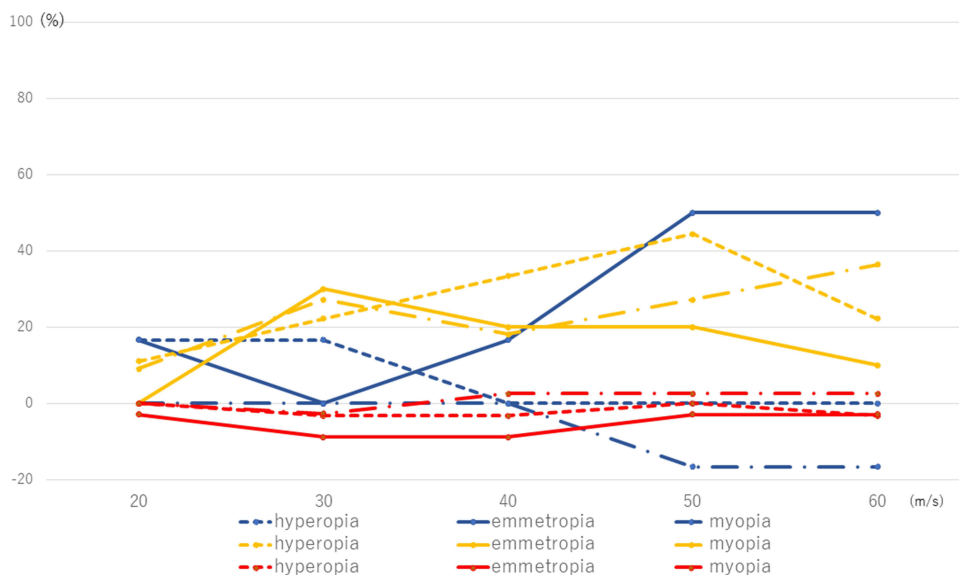


Figure 11 Deformation rate of anterior chamber, lens and vitreous for eyes with three axial lengths at 1.4 ms after airbag impact at five impact velocities. Legends pertaining to the line drawings are the same as in Figure 5.

that the vitreous body elongated posteriorly in an axial direction seems to support this hypothesis. Further simulation-based studies, including those conducted by our group in the equatorial direction, are underway.

Our study has several limitations. First, the vitreous was modeled as a solid mass, whereas age-related changes in the vitreous, with liquefaction and partial vitreous separation, alter the biomechanics of the vitreous,^{52,53} which may alter the pathology of vitreoretinal complications with airbag impact, similar to age-related changes in the physiological properties of the lens. In future studies, these factors should be considered to refine the simulation accuracy. Second, while deformation of the eye occurred in three dimensions with airbag impact, the intraocular segment deformation rate was analyzed in two dimensions using sequential axial change.

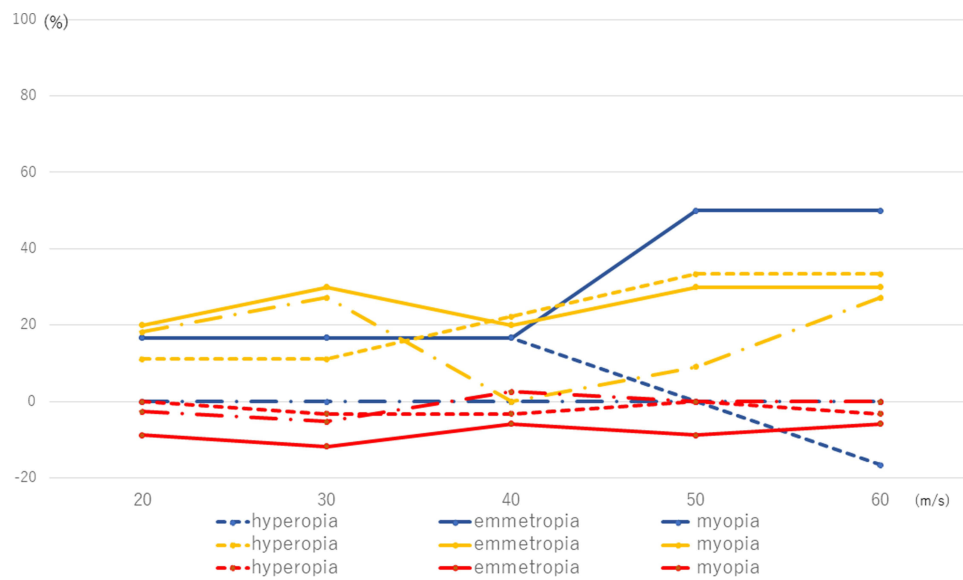


Figure 12 Deformation rate of anterior chamber, lens and vitreous for eyes with three axial lengths at 1.6 ms after airbag impact at five impact velocities. Legends pertaining to the line drawings are the same as in Figure 5.

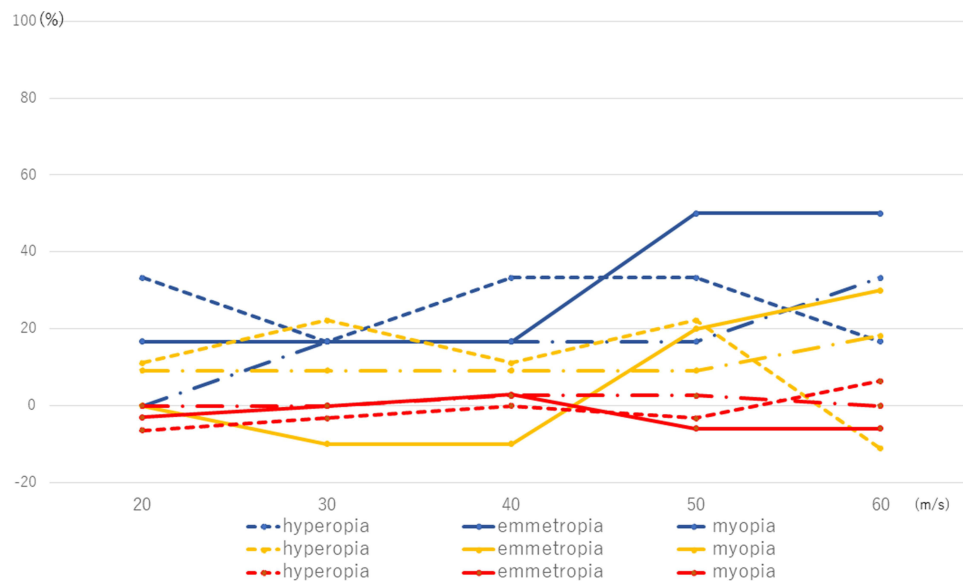


Figure 13 Deformation rate of anterior chamber, lens and vitreous for eyes with three axial lengths at 1.8 ms after airbag impact at five impact velocities. Legends pertaining to the line drawings are the same as in Figure 5.

Deformation in other directions is important, and useful information can be obtained by comparing this with the value in the axial direction. The sequential volume change in each segment was calculated to upgrade the analysis. Refinement of our simulation model for future studies is also underway.

Studies of intraocular deformation upon blunt airbag impact will be of interest to ophthalmologists. Study of trauma could provide insights into how the eye responds to impact injury and could also help the automobile industry make more adaptable airbags customized to prevent serious damage by changing the expansion process, and could also support the need for protective materials including eyeglasses to reduce the risk to the anterior segment of the eyeball.

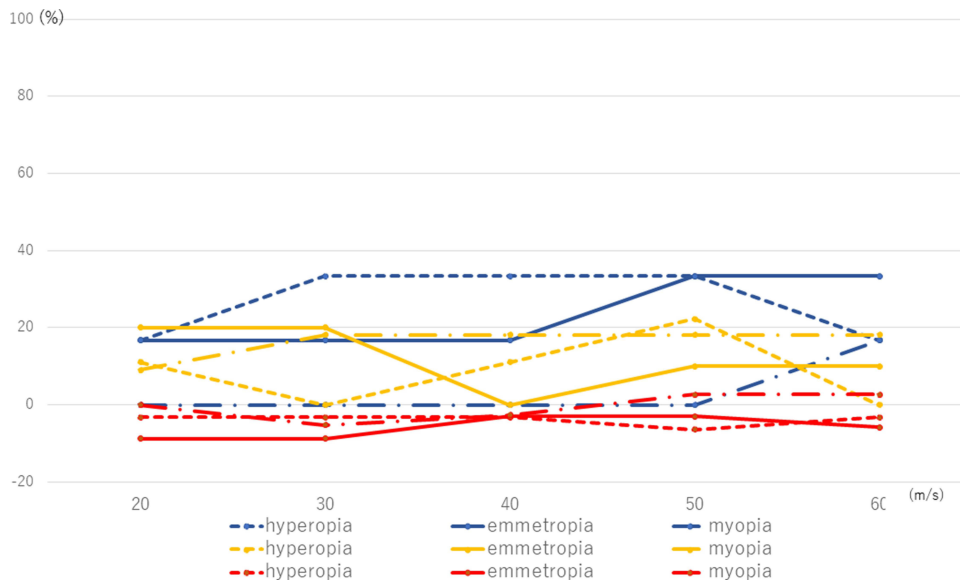


Figure 14 Deformation rate of anterior chamber, lens and vitreous for eyes with three axial lengths at 2.0 ms after airbag impact at five impact velocities. Legends pertaining to the line drawings are the same as in Figure 5.

Acknowledgments

This work was supported by a Grant-in-Aid for the Encouragement of Scientists (21K09709) from the Ministry of Education, Science, Sports and Culture of Japan. We thank Dr. W Gray for editing the manuscript.

Funding

The authors have no relevant financial or non-financial interests to disclose.

Disclosure

The authors report no conflict of interest in this work.

References

- Viano DC, King AI, Melvin JW, Weber K. Injury biomechanics research: an essential element in the prevention of trauma. *J Biomech.* 1989;22(5):403–417. doi:10.1016/0021-9290(89)90201-7
- Segui-Gomez M, Levy J, Roman H, Thompson KM, McCabe K, Graham JD. Driver distance from the steering wheel: perception and objective measurement. *Am J Public Health.* 1999;89(7):1109–1111. doi:10.2105/AJPH.89.7.1109
- Manche EE, Goldberg RA, Mondino BJ. Airbag-related ocular injuries. *Ophthalmic Surg Lasers.* 1997;28(3):246–250. doi:10.3928/1542-8877-19970301-15
- O'Halloran HS, Draud K, Stevens JL. Primary enucleation as a consequence of airbag injury. *J Trauma.* 1998;44(6):1090. doi:10.1097/00005373-199806000-00025
- de Vries S, Geerards AJ. Long-term sequelae of isolated chemical "airbag" keratitis. *Cornea.* 2007;26(8):998–999. doi:10.1097/ICO.0b013e3180ca9a35
- Baker RS, Flowers CW, Singh P, Smith A, Casey R. Corneoscleral laceration caused by airbag trauma. *Am J Ophthalmol.* 1996;121(6):709–711. doi:10.1016/S0002-9394(14)70639-7
- Scott IU, Greenfield DS, Parrish RK. Airbag-associated injury producing cyclodialysis cleft and ocular hypotony. *Ophthalmic Surg Lasers.* 1996;27(11):955–957. doi:10.3928/1542-8877-19961101-12
- Fukagawa K, Tsubota K, Kimura C, et al. Corneal endothelial cell loss induced by airbags. *Ophthalmology.* 1993;100(12):1819–1823. doi:10.1016/S0161-6420(13)31394-3
- Han DP. Retinal detachment caused by airbag injury. *Arch Ophthalmol.* 1993;111(10):1317–1318. doi:10.1001/archoph.1993.01090100023010
- Scott IU, John GR, Stark WJ. Airbag-associated ocular injury and periorbital fractures. *Arch Ophthalmol.* 1993;111(1):25. doi:10.1001/archoph.1993.01090010027016
- Vichnin MC, Jaeger EA, Gault JA, Jeffers JB. Ocular injuries related to airbag inflation. *Ophthalmic Surg Lasers.* 1995;26(6):542–548. doi:10.3928/1542-8877-19951101-09
- Onwuzuruigbo CJ, Fulda GJ, Larned D, Hailstone D. Traumatic blindness after airbag deployment: bilateral lenticular dislocation. *J Trauma.* 1996;40(2):314–316. doi:10.1097/00005373-199602000-00029

13. Ghafouri A, Burgess SK, Hrdlicka ZK, Zigelbaum BM. Airbag-related ocular trauma. *Am J Emerg Med.* 1997;15(4):389–392. doi:10.1016/S0735-6757(97)90135-2
14. Koisaari T, Leivo T, Sahraravand A, Haavisto A-H, Sulander P, Tervo TMT. Airbag deployment-related eye injuries. *Traffic Inj Prev.* 2017;18(5):493–499. doi:10.1080/15389588.2016.1271945
15. Wang SH, Lim CC, Teng YT. Airbag-associated severe blunt eye injury causes choroidal rupture and retinal hemorrhage: a case report. *Case Rep Ophthalmol.* 2017;8(1):13–20. doi:10.1159/000452652
16. Vohra V, Chawla H. Corneal endothelial decompensation due to airbag injury. *Int Ophthalmol.* 2018;38(5):2171–2174. doi:10.1007/s10792-018-0999-7
17. Leshner MP, Durrie DS, Stiles MC. Corneal edema, hyphema, and angle recession after air bag inflation. *Arch Ophthalmol.* 1993;111(10):1320–1322. doi:10.1001/archophth.1993.01090100026014
18. Ruiz-Moreno JM. Air bag-associated retinal tear. *Eur J Ophthalmol.* 1998;8(1):52–53. doi:10.1177/112067219800800112
19. Kaizu Y, Nakao S, Yamaguchi M, Murakami Y, Salehi-Had H, Ishibashi T. Detection of airbag impact-induced cone photoreceptor damage by adaptive optics scanning laser ophthalmoscopy: a case report. *BMC Ophthalmol.* 2016;16:99. doi:10.1186/s12886-016-0275-4
20. Savastano A, Donati MC, Rizzo S. Retinal tear related to air bag deployment. *JAMA Ophthalmol.* 2016;34(4):e155021. doi:10.1001/jamaophthol.2015.5021
21. Kung J, Leung LS, Leng T, Liao YJ. Traumatic airbag maculopathy. *JAMA Ophthalmol.* 2013;131(5):685–687. doi:10.1001/jamaophthol.2013.883
22. Geggel HS, Griggs PB, Freeman MI. Irreversible bullous keratopathy after air bag trauma. *Case Reports CLAO J.* 1996;22(2):148–150.
23. Zabriskie NA, Hwang IP, Ramsey JF, Crandall AS. Anterior lens capsule rupture caused by air bag trauma. *Am J Ophthalmol.* 1997;123(6):832–833. doi:10.1016/S0002-9394(14)71133-X
24. Blackmon SM, Fekrat S, Setlik DE, Afshari NA. Posterior dislocation of a crystalline lens associated with airbag deployment. *J Cataract Refract Surg.* 2005;31(12):2431–2432. doi:10.1016/j.jcrs.2005.08.050
25. Salam T, Stavrakas P, Wickham L, Bainbridge J. Airbag injury and bilateral globe rupture. *Am J Emerg Med.* 2010;28(8):982.e5–982.e6. doi:10.1016/j.ajem.2009.12.015
26. Elliott D, Hauch A, Kim RW, Fawzi A. Retinal dialysis and detachment in a child after airbag deployment. *J AAPOS.* 2011;15(2):203–204. doi:10.1016/j.jaapos.2010.11.021
27. Mohamed AA, Banerjee A. Patterns of injury associated with automobile airbag use. *Postgrad Med J.* 1998;74(874):455–458. doi:10.1136/pgmj.74.874.455
28. Duma SM, Kress TA, Porta DJ, Simmons RJ, Alexander CL, Woods CD. Airbag-induced eye injuries: experiments with in situ cadaver eyes. *Biomed Sci Instrum.* 1997;33:106–111.
29. Duma SM, Crandall JR. Eye injuries from airbags with seamless module covers. *J Trauma.* 2000;48(4):786–789. doi:10.1097/00005373-200004000-00036
30. Shirzadi H, Zohoor H, Naserkhaki S. Biomechanical simulation of eye-airbag impacts during vehicle accidents. *Proc Inst Mech Eng H.* 2018;232(7):699–707. doi:10.1177/0954411918778063
31. Power ED, Duma SM, Stitzel JD, et al. Computer modeling of airbag-induced ocular injury in pilots wearing night vision goggles. *Aviat Space Environ Med.* 2002;73(10):1000–1006.
32. Uchio E, Ohno S, Kudoh J, Aoki K, Kisielwicz LT. Simulation model of an eyeball based on finite element analysis on a supercomputer. *Br J Ophthalmol.* 1999;83(10):1106–1111. doi:10.1136/bjo.83.10.1106
33. Uchio E, Kadonosono K, Matsuoka Y, Goto S. Simulation of airbag impact on an eye with transsclerally fixated posterior chamber intraocular lens using finite element analysis. *J Cataract Refract Surg.* 2004;30(2):483–490. doi:10.1016/S0886-3350(03)00520-0
34. Uchio E, Ohno S, Kudoh K, Kadonosono K, Andoh K, Kisielwicz LT. Simulation of airbag impact on post-radial keratotomy eye using finite element analysis. *J Cataract Refract Surg.* 2001;27(11):1847–1853. doi:10.1016/S0886-3350(01)00966-X
35. Uchio E, Watanabe Y, Kadonosono K, Matsuoka Y, Goto S. Simulation of airbag impact on eyes after photorefractive keratectomy by finite element analysis method. *Graefes Arch Clin Exp Ophthalmol.* 2003;241(6):497–504. doi:10.1007/s00417-003-0679-8
36. Huang J, Uchio E, Goto S. Simulation of airbag impact on eyes with different axial lengths after transsclerally fixated posterior chamber intraocular lens by using finite element analysis. *Clin Ophthalmol.* 2015;9:263–270. doi:10.2147/OPHTH.S75180
37. Okamura K, Shimokawa A, Takahashi R, Saeki Y, Ozaki H, Uchio E. Finite element analysis of air gun impact on post-keratoplasty eye. *Clin Ophthalmol.* 2020;14:179–186. doi:10.2147/OPHTH.S236825
38. Takahashi R, Okamura K, Tsukahara-Kawamura T, et al. Finite element analysis of changes in tensile strain by airsoft gun impact on eye and deformation rate in eyes of various axial lengths. *Clin Ophthalmol.* 2020;14:1445–1450. doi:10.2147/OPHTH.S249483
39. Kobayashi A, Izaki R, Fujita H, et al. Finite element analysis of changes in tensile strain and deformation by airbag impact in eyes of various axial lengths. *Int Ophthalmol.* 2022;43(7):2143–2151. doi:10.1007/s10792-022-02609-7
40. Ruan JS, Prasad P. Coupling of a finite element human head model with a lumped parameter Hybrid III dummy model: preliminary results. *J Neurotrauma.* 1995;42(4):725–734. doi:10.1089/neu.1995.12.725
41. Hoeltzel DA, Altman P, Buzard K, Choe K. Strip extensimetry for comparison of the mechanical response of bovine, rabbit, and human corneas. *J Biomech Eng.* 1992;114(2):202–215. doi:10.1115/1.2891373
42. Reichel E, Miller D, Blanco E, Mastanduno R. The elastic modulus of central and perilimbal bovine cornea. *Ann Ophthalmol.* 1989;21(6):205–208.
43. Oliveira C, Harizman N, Girkin CA, et al. Axial length and optic disc size in normal eyes. *Br J Ophthalmol.* 2007;91(1):37–39. doi:10.1136/bjo.2006.102061
44. Kim JM, Kim KO, Kim YD, Choi GJ. A case of air-bag associated severe ocular injury. *Korean J Ophthalmol.* 2004;18:84–88.
45. Schreck RM, Rouhana SW, Santrock J, et al. Physical and chemical characterization of airbag effluents. *J Trauma.* 1995;38(4):528–532. doi:10.1097/00005373-199504000-00011
46. Pearlman JA, Au Eong KG, Kuhn E, Pieramici DJ. Airbags and eye injuries: epidemiology, spectrum of injury, and analysis of risk factors. *Surv Ophthalmol.* 2001;46(3):234–242. doi:10.1016/S0039-6257(01)00256-9
47. Stein JD, Jaeger EA, Jeffers JB. Air bags and ocular injuries. *Trans Am Ophthalmol Soc.* 1999;97:59–82.
48. Yang CS, Chou TF, Liu JH, Hsu WM. Air bag associated posterior segment ocular trauma. *J Chin Med Assoc.* 2004;67(8):425–431.

49. Madreperla SA, Benetz BA. Formation and treatment of a traumatic macular hole. *Arch Ophthalmol*. 1997;115(9):1210–1211. doi:10.1001/archophth.1997.01100160380026
50. Delori F, Pomerantzeff O, Cox MS. Deformation of the globe under high speed impact: its relation to contusion injuries. *Invest Ophthalmol*. 1969;8(3):290–301.
51. Weidenthal DT, Schepens CL. Peripheral fundus changes associated with ocular contusion. *Am J Ophthalmol*. 1966;62(3):465–477. doi:10.1016/0002-9394(66)91326-2
52. Walton KA, Meyer CH, Harkrider CJ, Cox TA, Toth CA. Age-related changes in vitreous mobility as measured by video B scan ultrasound. *Exp Eye Res*. 2002;74(2):173–180. doi:10.1006/exer.2001.1136
53. Ruminski D, Sebag J, Toledo RD, et al. Volumetric optical imaging and quantitative analysis of age-related changes in anterior human vitreous. *Invest Ophthalmol Vis Sci*. 2021;62(4):31. doi:10.1167/iovs.62.4.31

Clinical Ophthalmology

Dovepress

Publish your work in this journal

Clinical Ophthalmology is an international, peer-reviewed journal covering all subspecialties within ophthalmology. Key topics include: Optometry; Visual science; Pharmacology and drug therapy in eye diseases; Basic Sciences; Primary and Secondary eye care; Patient Safety and Quality of Care Improvements. This journal is indexed on PubMed Central and CAS, and is the official journal of The Society of Clinical Ophthalmology (SCO). The manuscript management system is completely online and includes a very quick and fair peer-review system, which is all easy to use. Visit <http://www.dovepress.com/testimonials.php> to read real quotes from published authors.

Submit your manuscript here: <https://www.dovepress.com/clinical-ophthalmology-journal>